Schlieren measurements of the pressure wave induced by low energy electrical discharges

S. Essmann*, [1], D. Markus[1], U. Maas[2]

[1]Physikalisch-Technische Bundesanstalt, Braunschweig, Germany
[2]Karlsruhe Institute of Technology, Karlsruhe, Germany

Abstract

In this work, we investigate the pressure wave and the hot gas kernel originating from a low energy electrical discharge. A phase averaged schlieren setup was employed to determine the radii experimentally through analysis of the intensity profiles. The radial locations were also calculated using one-dimensional numerical simulations of the processes following the discharge. The fraction of rapid gas heating was considered by introducing an efficiency factor for the discharge energy. By comparison of the measured and simulated extensions of the kernel the efficiency of the discharge could be estimated.

Introduction

In safety relevant scenarios, electrical discharges are a frequently observed ignition source. A number of studies investigated the ignition process caused by electrical discharges with experimental and numerical methods, e.g. [1–4]. However, the discharge energies in automotive or aerospace applications are higher than those relevant to safety engineering problems. The minimum ignition energy (MIE) of many combustible gas/air mixtures is in the energy range from 20 to 1000 µJ. In this study we investigated such low energy discharges that play a role in safety relevant applications.

In an electrical discharge, energy is transferred from a capacitor into a rather small gas volume. A certain amount of heating occurs rapidly, within tens to hundreds of nanoseconds. The fraction of rapid heating in relation to the total heating can be viewed as an efficiency η [5–8]. Between the electrodes, the fast heating forms a nearly cylindrically shaped kernel. Here, the temperature and pressure are highly elevated compared to the gas outside the kernel; thus, the kernel expands at high velocity. On the perimeter a shock wave forms and detaches from the kernel after several 100 ns. The shock wave propagates into the surrounding gas, becoming spherical in shape and decaying into a pressure wave (or sound wave). The characteristics of the discharge affect the development of both the pressure wave and the kernel. Therefore, their radial locations at a specific point in time hold information about the discharge, for instance about the discharge energy and the energy density. In this study we determined the radii experimentally by schlieren imaging and numerically through one-dimensional simulations. By comparison of the data it is possible to assign an efficiency to the discharges. This efficiency accounts for all kinds of losses without distinguishing between the individual types.

Experimental Setup

Low energy electrical discharges were generated in air and burnable gas/air mixtures at atmospheric pressure and 21.0 ± 0.5 °C ambient temperature. They occurred between two tungsten electrodes 2.4 mm in diameter with rounded tips that were located in a cylindrical stainless steel vessel. The electrode distance L_s was 0.5 to 1.5 mm. The discharge energy E_s can be approximated by the energy stored on the capacitor, $E_s = 1/2\ CU^2$, where C is the capacitance of the setup (including stray capacitance) and U represents the breakdown voltage. In order to achieve repeatable discharges, we slowly increased the voltage across the gap at 0.02 kV/s using a remote controlled *FUG HCP 35-35000* high voltage source and an *Agilent 33500B* waveform generator. This yielded breakdown voltage variations smaller than 2%.

Single shot images of the pressure wave and the hot gas kernel were taken using a schlieren setup. A *Nanolite KL-L* flash lamp which had a flash duration of less than 25 ns was used as a light source. The light from the flash lamp was focused onto a rectangular slit and then

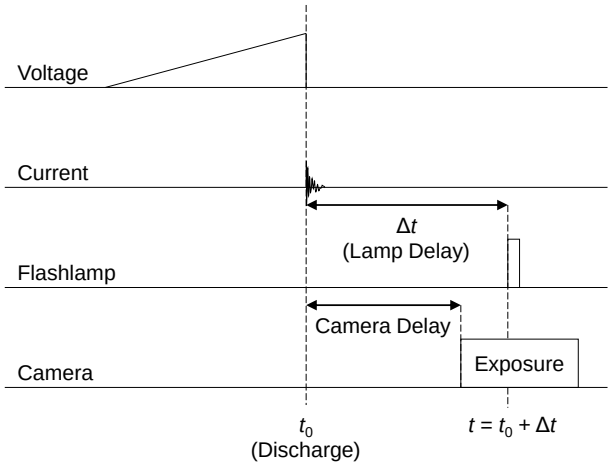

Figure 1: Timing diagram.

Table 1: Experimental setup for burnable gas/air mixtures.

Gas	Conc. / vol. %	L_s / mm	E_s / µJ
Propane	5.2	1.7	244
Ethylene	8.0	1.2	101

* Corresponding author: stefan.essmann@ptb.de

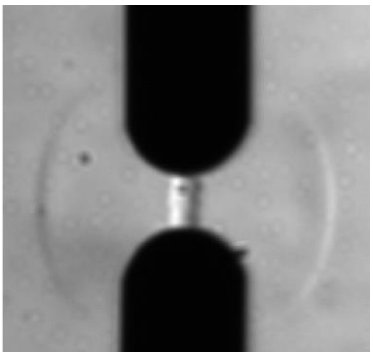

Figure 2: Sample schlieren image of the pressure wave and the kernel for case L_s = 1.0 mm, E_s = 87.0 µJ, taken 6.70 µs after the discharge.

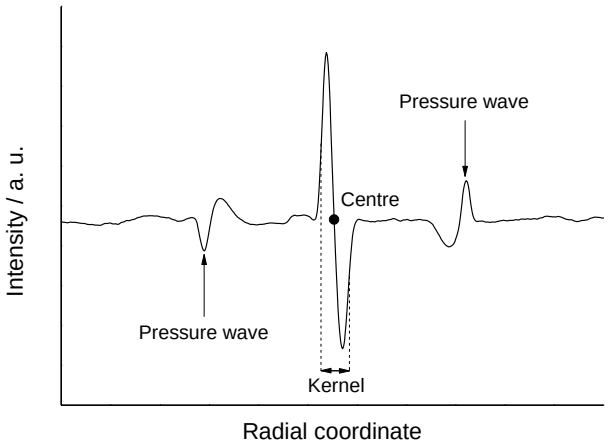

Figure 3: Intensity profile across the radial coordinate (horizontal in fig. 2). The great peaks in the centre correspond to the hot gas kernel while the smaller ones relate to the pressure wave.

parallelised by a 500 mm collimating lens. Behind the vessel, it was focused by another 500 mm collimating lens and cut off using a knife edge. The images were recorded by a *LaVision ImagerProPlus 2M* CCD camera with a spatial resolution of 54 pixel/mm. Since it was not known a priori when the discharge will occur, both the flash lamp and the camera were triggered by a *Quantum Components Model 9500* delay generator. The intrinsic delays of the camera and the flash lamp added to the chosen delay. Images could thus only be taken at times $t >$ 6.5 µs, where t_0 is the beginning of the discharge identified by the rising current across the electrodes (fig. 1). A *Yokogawa DL6154* oscilloscope recorded the discharge current, breakdown voltage, and time of flash lamp trigger.

We carried out measurements in air for varying energies at two fixed electrode distances (0.5 mm and 1.0 mm). Regarding the burnable gas/air mixtures we investigated propane and ethylene in near MIE conditions. Details may be found in Table 1.

Three images were taken for each instant in every configuration to determine the repeatability of the measurements. Figure 2 shows a sample schlieren image of the heated gas kernel and the pressure wave. The images were processed by means of linear filtering and background subtraction. Then a horizontal intensity profile from halfway between the electrodes was extracted. From this we found the centre point as well as the positions of the kernel and the pressure wave (fig. 3).

Numerical Simulation

A as can be seen in fig. 2 the spark discharge can be represented by a one-dimensional description by means of a cylindrical geometry. The shock wave is cylindrical in the beginning but develops into a spherical wave at longer distances which is not covered from the numerical simulations. However, even though a cylindrical pressure wave undergoes less decay than a spherical one, this error could be neglected at the early stage. Here, the spark is described as an infinite cylinder with radius r_s and the simulations were performed perpendicular to the spark channel. The solutions of the well-known mass, species, momentum, and energy equations were obtained using a time integration method [9]. For the simulation of an ignition of ethylene/air mixtures a detailed C4-mechanism of 53 species and 592 elementary reactions given by Chevalier [10] is used.

The initial conditions for the calculations were those of a quiescent, homogeneous air mixture. The boundary conditions were zero gradients at the inner and outer boundary. The vessel was represented numerically using a constant outer radius of 5 cm and a constant wall temperature. Plasma effects are neglected, hence, the numerical representation considers only the local heating of the gas inside the ignition volume using a source term q in the energy conservation equation. The energy deposition term is given by [11]

$$q = \begin{cases} \frac{D_s}{t_s} \exp\left(-\left(\frac{r}{r_s}\right)^8\right) & \text{for } 0 \le t \le t_s \\ 0 & \text{for } t > t_s \end{cases},$$

where D_s represents the spark energy density deposited during the spark duration t_s = 500 ns given by $D_s = \eta \cdot E_s/(L_s \cdot \pi r_s^2)$. Here, r_s represents the spark radius (r_s = 200 µm when not stated otherwise). An efficiency factor η is used to consider the fraction of rapid gas heating as has been done in other works [5–8].

Heat losses to the electrodes and plasma processes like the breakdown phase are not considered directly in this work, since this would require a two-dimensional approach [12]. Using the experimentally given spark duration, spark channel length, and spark energy the efficiency factor was varied to examine the kernel growth and pressure wave propagation. These are yielded from the temporal evolution of the density profiles in correspondence to the experimental method described above.

Results and Discussion

Figure 4 shows the radial development of the pressure wave and the kernel in air at a constant electrode distance for varying discharge energies. A strong dependence on the discharge energy is evident. An increase in discharge energy yields larger pressure wave radii. Due to the missing data at early times ($t <$ 6.5 µs), we cannot know whether the pressure wave and kernel start at the same

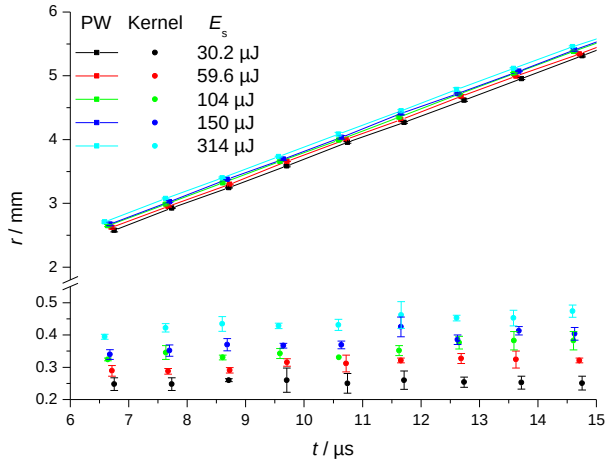

Figure 4: Experimentally determined pressure wave and kernel radii at varying discharge energies at L_s = 0.5 mm.

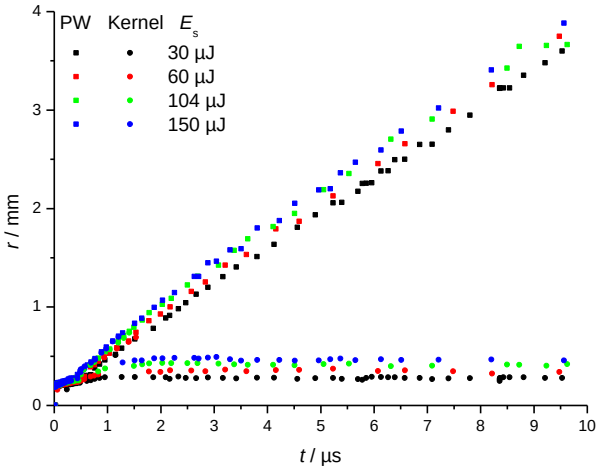

Figure 5: Simulated radial locations of the pressure wave (PW) and the kernel for L_s = 0.5 mm.

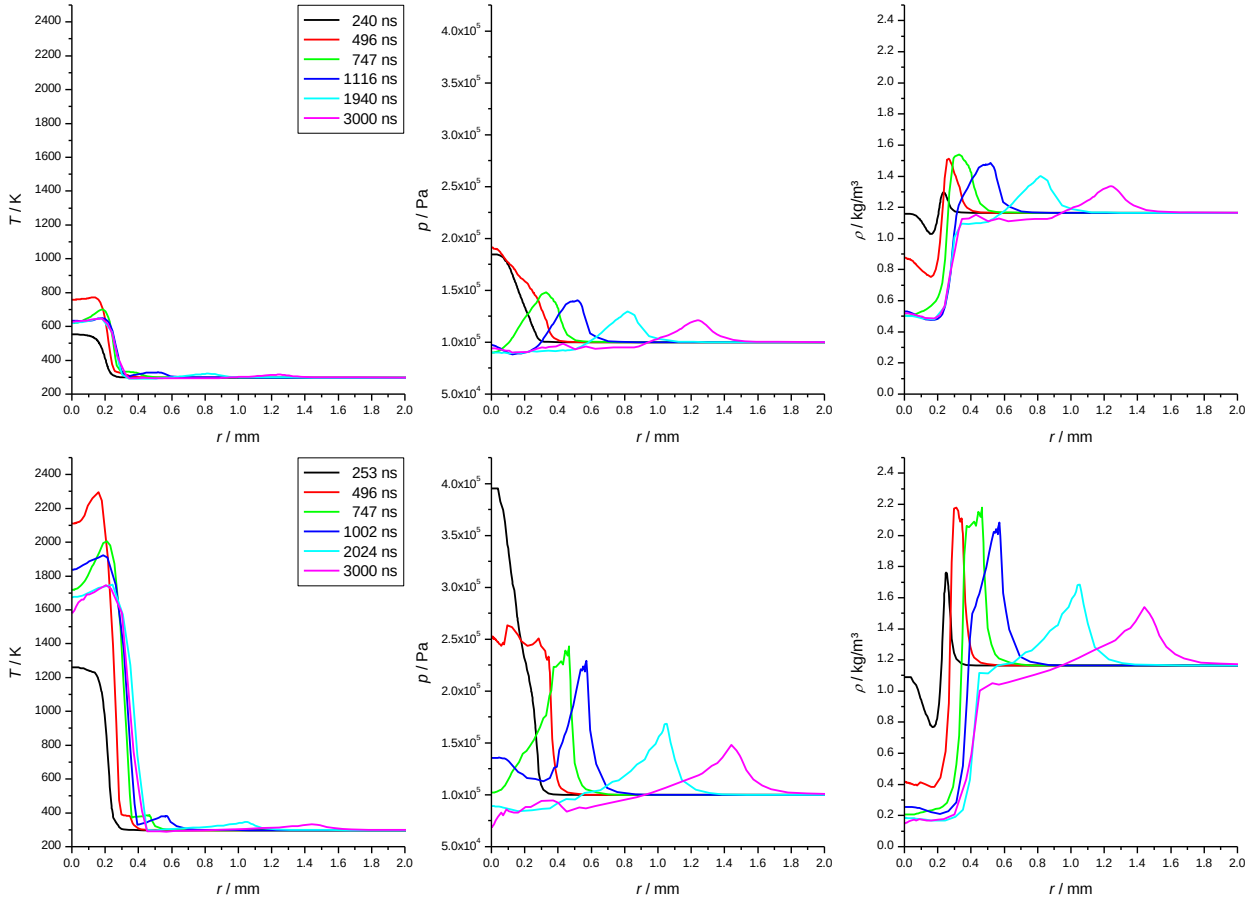

Figure 6: Radial profiles of temperature, pressure, and density (from left to right) for L_s = 0.5 mm, E_s = 104 µJ. Efficiency $\eta = 0.25$ (top row) and $\eta = 1.0$ (bottom row).

radius for varying energy, nor at what time the curves of different energy separate. The speed of the pressure wave does not depend on the discharge energy in the accessible time range. It is slightly above sound speed for all cases. The radius of the hot gas kernel also rises at higher discharge energy. In the lower energy cases no significant growth is observed whereas at greater energy the kernel radius still increases. The kernel radius apparently approaches a constant value that increases with discharge energy.

The numerical simulation captures these trends well (fig. 5). Detachment of the shock wave from the kernel can be seen after several 100 ns. The initial velocity of the expansion is higher at greater discharge energy. This leads to a separation of the pressure wave curves of different energy within 1 µs. After about 3 µs the

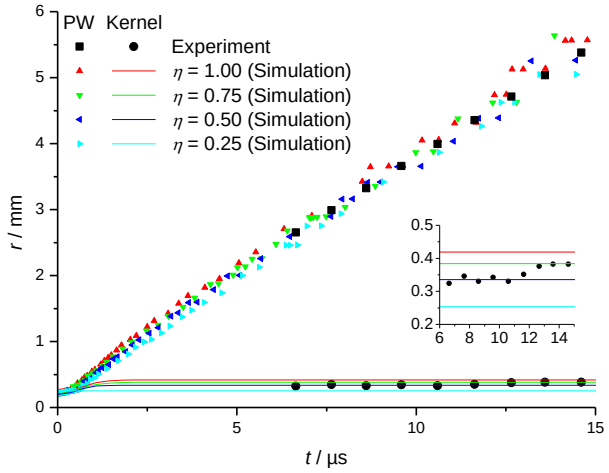

Figure 7: Effect of η on the kernel and pressure wave for case L_s = 0.5 mm, E_s = 104 µJ.

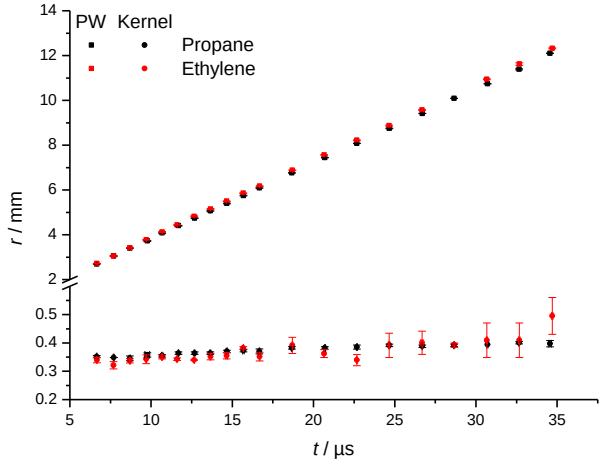

Figure 8: Pressure wave (PW) and kernel radii for the propane and ethylene cases (details are given in Table 1).

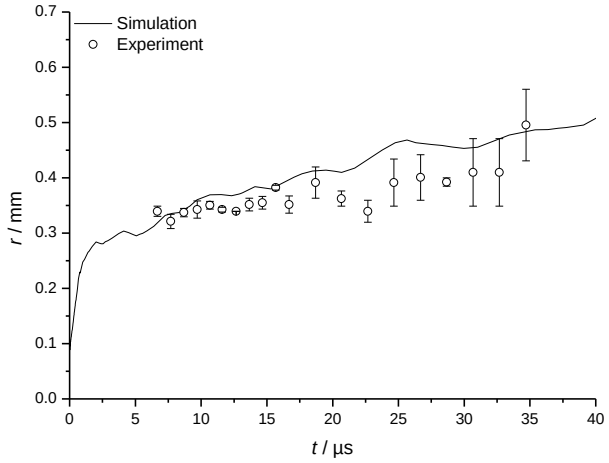

Figure 9: Radial position of the hot kernel for the ethylene/air mixture. The spark radius r_s for the simulation was 100 µm.

pressure wave curves become parallel, reproducing the observation in the experiment. The kernel growth due to hot gas expansion is rapid in the first microsecond after the beginning of the discharge and then gradually slows down. It is nearly finished within about 2 µs in the simulations whereas some growth is still observed at later times in the experiments. This may be due to two-dimensional fluid dynamic effects like recirculation at the electrode tips that are not resolved in this numerical description [12, 13].

These effects can be explained by taking a look at the simulated radial profiles of temperature, pressure, and density at different time steps for varying efficiencies η (fig. 6). Greater efficiency results in more energy being rapidly transformed into heat in the spark channel. The first two time steps up to about 500 ns shown in fig. 6 show the heating of the gas due to the discharge, leading to a maximum temperature of about 750 K in the low efficiency ($\eta = 0.25$, top row) and 2300 K high efficiency ($\eta = 1.0$, bottom row) case, respectively. During these very first stages a fast pressure rise can be seen. The pressure peak is significantly greater in the high efficiency case and is reached at an earlier time. The growth of the hot kernel is driven by pressure at these early times; the heat flux time scale is much larger. At high efficiency, the pressure in the centre is already decreasing after 500 ns due to the fast expansion of the kernel while at lower efficiency it takes longer for the pressure in the centre to decrease. Hence, the kernel expansion which can best be monitored in the density profile is faster at high efficiency. The pressure gradient is steep enough to cause a shock wave to form. Detachment of the shock wave from the heated kernel can be seen after 700 to 1000 ns in the pressure and density profiles. It occurs earlier at high efficiency which can also be seen in fig. 5.

Figure 7 shows experimental data for the case L_s = 0.5 mm, E_s = 104 µJ in air and compares this to numerical simulations with varying efficiency η. Comparing the experimental and numerical radial development of the kernel, $\eta \approx 0.5$ matches the experimental data best (see inset). For the fraction of energy that contributes to rapid gas heating, smaller values are found in the literature; for example, Xu et al. [8] report $\eta = 0.2-0.25$ for a case that features repetitively pulsed discharges at 1 kHz at similar energy and ambient conditions. Popov [5] numerically found $\eta = 0.28$ over a wide range of reduced electric field values.

Figure 8 shows the measured pressure wave and kernel radii for the propane/air and ethylene/air mixtures. The pressure waves propagate at close to the corresponding sound speed. In the experimentally accessible time range, the kernel expansion is slow but not negligible. The kernel propagation is about equal for both mixtures though the energy is more than twice as high in the propane/air case. An extension of the experimentally accessible time range is needed in order to resolve this question.

Additionally, the propagation of the hot gas kernel was simulated for the ethylene/air case. The results are shown in fig. 9. The calculation was performed with $r_s = 100\,\mu m$. The simulation matches the experimentally obtained data well. In contrast to the simulations performed in air, the kernel continues to grow even after the pressure-driven expansion is completed due to the ignition that has taken place. Here, the kernel has become a flame kernel.

Conclusion

Using a phase resolved schlieren setup we measured the radii of the pressure wave and the hot gas kernel induced by low energy electrical discharges. The data was compared to one-dimensional numerical simulations which reproduced the same trends. Using calculated profiles of temperature, pressure, and density, the experimentally yielded results could be explained.

We used an efficiency factor in the simulations that indicates the fraction of energy which rapidly heats the gas. For the investigated case in air it was found to be approximately 0.5. Future work will need to include further parameters so as to quantify certain losses. This is intended to result in a detailed energy balance of low energy electrical discharges.

Experiments and simulations were performed for two safety relevant cases in ethylene/air and propane/air at near MIE conditions. The pressure wave propagation speed was determined to be close to sound speed. Good agreement regarding the kernel evolution was achieved.

In future work we plan to modify the experimental setup in order to measure the radii at earlier times, since the kernel expands rapidly in the first few microseconds. On the numerical side, two-dimensional simulations could consider for instance a less idealised geometry or fluid dynamic effects.

Acknowledgements

The authors would like to acknowledge funding from the Deutsche Forschungsgemeinschaft (DFG) under grant FOR1447.

References

[1] D.R. Lintin, E.R. Wooding, Investigation of the ignition of a gas by an electric spark, Br. J. Appl. Phys. 10 (1959) 159.

[2] R. Maly, Ignition model for spark discharges and the early phase of flame front growth, Symp. (Int.) on Combustion 18 (1981) 1747–1754.

[3] D. Bradley, F.K.-K. Lung, Spark ignition and the early stages of turbulent flame propagation, Combust. Flame 69 (1987) 71–93.

[4] P.L. Pitt, R.M. Clements, D.R. Topham, The Early Phase of Spark Ignition, Combust. Sci. and Tech. 78 (1991) 289–314.

[5] N.A. Popov, Investigation of the mechanism for rapid heating of nitrogen and air in gas discharges, Plasma Phys. Rep. 27 (2001) 886-896.

[6] N.L. Aleksandrov, S.V. Kindysheva, M.M. Nudnova, A.Y. Starikovskiy, Mechanism of ultra-fast heating in a non-equilibrium weakly ionized air discharge plasma in high electric fields, J. Phys. D: Appl. Phys. 43 (2010) 255201.

[7] D.L. Rusterholtz, D.A. Lacoste, G.D. Stancu, D.Z. Pai, C.O. Laux, Ultrafast heating and oxygen dissociation in atmospheric pressure air by nanosecond repetitively pulsed discharges, J. Phys. D: Appl. Phys. 46 (2013) 464010.

[8] D.A. Xu, M.N. Shneider, D.A. Lacoste, C.O. Laux, Thermal and hydrodynamic effects of nanosecond discharges in atmospheric pressure air, J. Phys. D: Appl. Phys. 47 (2014) 235202.

[9] U. Maas, J. Warnatz, Ignition Processes in Hydrogen-Oxygen Mixtures, Combust. Flame 74 (1988) 53–69.

[10] C. Chevalier, Entwicklung eines detaillierten Reaktionsmechanismus zur Modellierung der Verbrennungsprozesse von Kohlenwasserstoffen bei Hoch- und Niedertemperaturbedingungen. PhD Thesis, Stuttgart University, 1993.

[11] A. Dreizler, S. Lindenmaier, U. Maas, J. Hult, M. Aldén, C.F. Kaminski, Characterisation of a spark ignition system by planar laser-induced fluorescence of OH at high repetition rates and comparison with chemical kinetic calculations, Appl. Phys. B 70 (2000) 287–294.

[12] M. Thiele, J. Warnatz, A. Dreizler, S. Lindenmaier, R. Schießl, U. Maas, A. Grant, P. Ewart, Spark Ignited Hydrogen/Air Mixtures: Two Dimensional Detailed Modeling and Laser Based Diagnostics, Combust. Flame 128 (2002) 74–87.

[13] S.P. Bane, J.L. Ziegler, J.E. Shepherd, Investigation of the effect of electrode geometry on spark ignition, Combust. Flame 162 (2015) 462–469.